X-RAY SOURCES IN REGIONS OF STAR FORMATION. II. THE PRE-MAIN-SEQUENCE G STAR HDE 283572

F. M. Walter^{1,2,3}

Center for Astrophysics and Space Astronomy, University of Colorado

A. Brown⁴ and J. L. Linsky^{2,5}

Joint Institute for Laboratory Astrophysics, University of Colorado and National Bureau of Standards

A. E. RYDGREN¹

Astronomy Program, Computer Sciences Corporation

F. VRBA¹

United States Naval Observatory, Flagstaff Station

M. ROTH AND L. CARRASCO

Instituto de Astronomia, Universidad Nacional Autónoma de Mexico

P. F. CHUGAINOV AND N. I. SHAKOVSKAYA Crimean Astrophysical Observatory

AND

C. L. IMHOFF²

Astronomy Program, Computer Sciences Corporation Received 1986 June 23; accepted 1986 August 25

ABSTRACT

We have detected HDE 283572, a ninth-magnitude G star 8' south of RY Tau, as a bright X-ray source, and subsequent observations have revealed it to be one of the brightest late-type pre-main-sequence stars. It has a rotation period of 1.5 and strong chromospheric and coronal emission yet no evidence for an IR excess or a strong stellar wind. Ha is in absorption. The Li abundance is cosmic. We conclude that HDE 283572 is a 2 M_{\odot} naked T Tauri star. We have calculated simple models of the outer atmospheric structure of HDE 283572 based on the observed ultraviolet and X-ray emission measures. The transition region electron density is $\sim 2 \times 10^{10}$ cm⁻³ at log $T_e = 4.75$, based on density-sensitive line ratios. Models that combine the X-ray and UV data result in transition region pressures more than one order of magnitude larger than the observed value, suggesting that the dominant coronal and transition region emitting regions are physically distinct. Models based solely on the UV data give pressures in agreement with the observed value. The total radiative losses from regions with electron temperatures between 10^4 and 2×10^5 K are 2.9×10^8 ergs cm⁻² s⁻¹, which is $\sim 10^3$ times the equivalent quiet Sun value.

Subject headings: stars: chromospheres — stars: formation — stars: individual — stars: pre-main-sequence — stars: X-rays

I. INTRODUCTION

The Taurus-Auriga T association is a few million years old (Cohen and Kuhi 1979). Low-mass stars in this association should lie well above the main sequence and, if not embedded, should be seen as T Tauri stars. The association is too young for the stars to have become post—T Tauri (PTT) stars, as defined by Herbig (1978). Nevertheless, there is a sizable population of young, active low-mass stars which are not T Tauri stars in the Tau-Aur T association.

Feigelson and Kriss (1981) and Walter and Kuhi (1981) discovered five relatively inactive low-mass pre-main-sequence (PMS) stars in the Tau-Aur region. Mundt et al. (1983) concluded that these stars had all the attributes of PTT stars

except that their ages were indistinguishable from those of T Tauri stars of comparable masses. Walter (1986) suggested that a better classification for these stars is "naked T Tauri" (NTT) stars, i.e., stars identical to the low-mass T Tauri stars save for the lack of a significant circumstellar envelope and resulting IR excess and $H\alpha$ emission from the cool, extended material. It was postulated that the existence of the circumstellar material observed around T Tauri stars was a consequence of the dusty environment wherein they reside, while the NTT stars, having moved out of their natal clouds into low-density interstellar space, have dissipated their circumstellar envelopes.

In addition to the five late-type stars discussed above, HDE $283572 (=BD + 27^{\circ}657 = SAO 76567)$, another X-ray bright non–T Tauri star in the Tau-Aur region, was discovered in the Einstein data. We first noted this star as a bright serendipitously discovered X-ray source near RY Tau (Walter and Kuhi 1981). Here we present a detailed discussion of observations at wavelengths ranging from X-ray to near-infrared, which demonstrate the PMS nature of HDE 283572 and show that it is likely to be a relatively high-mass NTT star, possibly the predecessor of an A dwarf star.

¹ Visiting Astronomer, Kitt Peak National Observatory, which is operated by the Association of Universities for Research in Astronomy, Inc., under contract with the National Science Foundation.

² Guest Observer with the International Ultraviolet Explorer.

³ Guest Observer with the Einstein Observatory.

⁴ Guest Observer with the EXOSAT Observatory.

⁵ Staff Member, Quantum Physics Division, National Bureau of Standards.

II. OBSERVATIONS AND DATA REDUCTION

a) X-Rays

HDE 283572 has been observed at X-ray wavelengths on three occasions. We noted it as the strongest X-ray source in *Einstein* Imaging Proportional Counter (IPC) image 4507 obtained on 1980 February 22 from 0:34 to 1:48 UT. (The *Einstein Observatory* and the IPC are described by Giacconi *et al.* 1979.) Sequence 4507 was centered on the T Tauri star RY Tau (Walter and Kuhi 1981); HDE 283572 was 8' off-axis. HDE 283572 was reobserved 3h later, in sequence 3843, centered on DE Tau. The second exposure ran from 3:43 to 4:57 UT with HDE 283572 23' off-axis.

We reobserved the RY Tau region with the *EXOSAT* Channel Multiplier Arrays (CMA; de Korte *et al.* 1981) on 1983 October 17 from 0905 to 1212 UT. HDE 283572 was within the CMA field of view, but was not detected, with a 3 σ upper limit of 0.013 counts s⁻¹ in the thin Lexan filter.

b) Photometry

HDE 283572 was monitored with *UBVRI* photometry over a 16 night interval during 1983 October from the Crimean Astrophysical Observatory, the US Naval Observatory Flagstaff Station, and the Mexican National Astronomical Observatory (MNAO). Details of Crimean and Flagstaff observing and reduction procedures appear in Vrba *et al.* (1986). The observations from MNAO were obtained with the 84 cm telescope and an RCA 31034-A photomultiplier.

We have averaged the results from each observatory for each night to reduce the effects of random photometric errors. This is necessary because the amplitude of the V magnitude variations is ~ 0.1 mag. These averaged results are presented in Table 1.

The Crimean and Flagstaff observations used the same secondary standard star BD $+30^{\circ}659$. The Crimean V magnitudes are systematically 0.02 mag fainter than the Flagstaff V magnitudes because of disagreement over the V magnitude of

TABLE 1

V PHOTOMETRY OF HDE 283572

JD 2,445,600+	Sitea	V mag	n ^b
14.498	CAO	9.06	3
15.460	CAO	9.07	3
16.461	CAO	8.98	3
17.424	CAO	9.04	3
18.978	USNO	9.09	1
19.458	CAO	8.98	3
19.879	USNO	9.05	2
20.451	CAO	9.09	3
20.914	USNO	8.985	2
22.402	CAO	8.99	2
23.398	CAO	9.10	2
23.922	MNAO	9.045	4
24.410	CAO	9.01	2
25.429	CAO	9.01	2
25.896	MNAO	9.02	4
26.582	CAO	9.10	1
26.879	MNAO	9.05	3
27.899	MNAO	9.07	5
27.959	USNO	9.10	1
28.929	USNO	8.995	2

a CAO—Crimean Astrophysical Observatory; USNO—US Naval Observatory; MNAO— Mexican National Astronomy Observatory.

b Number of observations in the mean.

TABLE 2

Mean Photometric Indices of
HDE 283572

Index	Value	Index	Value
V	9.04	K	6.93
U-B	0.32	J-H	0.42
B-V	0.83	H-K	0.11
$V-R_1$	0.70	K-L	0.08
$V-I_J$	1.21	•••	•••

this standard. We have corrected the Crimean V magnitudes by -0.01 mag and corrected the Flagstaff V magnitudes +0.01 mag to facilitate comparison with the MNAO results.

We obtained JHKL photometry of HDE 283572 on 1983 October 16 and 18–21 using the infrared photometer described by Roth et al. (1984) on the 2.1 m telescope of the Observatorio Astronomico Nacional and on 1983 December 29 with the "Otto" InSb detector and a 15" aperture on the KPNO 1.3 m telescope.

The observed magnitude range is too small to permit significant detection of color variations. We present the mean photometric indices in Table 2. The observed infrared colors clearly show that this star lacks the warm $(T \approx 1300 \text{ K})$ circumstellar dust which characterizes the classical T Tauri stars.

c) Ultraviolet Spectroscopy

We obtained ultraviolet spectra of HDE 283572 on 1982 October 9 and 11 with the International Ultraviolet Explorer (IUE; Boggess et al. 1978). The low-dispersion SWP spectrum $(\lambda\lambda 1100-2000)$ has ~ 6 Å spectral resolution; the highresolution LWR spectrum ($\lambda\lambda 1900-3300$) has ~ 0.25 Å resolution. Both spectra are somewhat underexposed with maximum signals ~ 140 DN. The data were reduced using the standard IUE SIPS software, the 1980 May low-resolution flux calibrations (Bohlin and Holm 1980) and the Cassatella et al. (1980) LWR-HI calibrations and echelle ripple corrections. The data were analyzed at the Colorado Regional Data Analysis Facility (RDAF). In addition, we obtained four IUE low-resolution long-wavelength (LWR-LO) spectra of HDE 283572 between 1983 October 8-15, to monitor the Mg II emission and UV continuum flux. These data were reduced at the Goddard RDAF. The observations are summarized in Table 3.

d) Optical Spectroscopy

Between 1980 July and 1981 February we obtained a number of spectra of this star using the IDS (Robinson and Wampler 1972) on the Lick Observatory 1 m Nickel refractor. The 7500 Å blaze grating was used with a $CuSO_4$ order sorter in second order in the blue ($\lambda\lambda 3600-4800$; resolution ~ 2.5 Å)

TABLE 3

IUE OBSERVATION LOG

Image	Dispersion	Date	Exposure Time (minutes)
SWP 18244	Low	1982 Oct 9	440
LWR 14388	High	1982 Oct 11	240
LWR 16946	Low	1983 Oct 8	10
LWR 16961	Low	1983 Oct 10	20
LWR 16971	Low	1983 Oct 13	20
LWR 16979	Low	1983 Oct 15	17.5

No. 1, 1987 HDE 283572 299

and also unfiltered in first order centered on $\lambda 6500$ (resolution ~ 5 Å). The spectral coverage is ~ 2400 Å in first order. An 8".1 aperture was used. The data were flat-fielded using a quartz lamp to remove tube irregularities, and the background was subtracted. Because of the generally poor signal to noise, we did not further reduce these spectra and used them only for spectral classification.

On 1980 September 29, we obtained a coudé spectrum, plate EC 16942, with the Lick Observatory 3 m telescope using the 51 cm camera (16 Å mm⁻¹ reciprocal dispersion). The plate was digitized on the Berkeley PDS.

We also obtained nine spectra in the blue ($\lambda\lambda 3750-4250$) and three in the red ($\lambda\lambda6000-7000$) between 1982 August and 1985 October at Kitt Peak (KPNO) on the 2^m1 IIDS system. Using grating 36 (1200 l mm⁻¹), the 6" aperture, and either the CuSO₄ or GG 495 order sorters, the resolutions obtained were 1.7 Å (blue) or 3.7 Å (red). We used the IRS flux standards and the standard IPPS reduction package to reduce the data to flux versus wavelength. Because the nights, in general, were not photometric, we used the relation between stellar surface flux between 3925 and 3975 Å and the V-R color (Linsky et al. 1979) to place the reduced fluxes on an absolute scale, with $\sim \pm 15\%$ estimated accuracy (blue spectra only). E. Feigelson observed the Ca II infrared triplet region of HDE 283572 for us on 1983 October 16, using the Black Moshannon Observatory fiber-coupled spectrograph (Ramsey, Barden, and Nations 1980). R. Mathieu has obtained high-resolution spectra $(\lambda/\Delta\lambda = 24,000)$ of the $\lambda 5200$ region using the F. L. Whipple and Oak Ridge Observatory 1.5 m telescopes. The radial and rotational velocities have been measured by cross correlation with a template star (Wyatt 1985).

III. CHARACTERISTICS OF HDE 283572

a) Colors and Spectral Type

We have used the optical and infrared photometry, spectroscopy, and spectrophotometry to determine the spectral type and radius of the star.

The Lick 1 m IDS and KPNO IIDS spectra provide an estimate of the spectral type by comparison of line ratios with MK standards. The $\lambda 4325$:H γ ratio indicates a spectral type near G5, while the Sr I $\lambda 4077$ line is deeper than in a G5 dwarf. The other lines between ~ 4000 and ~ 4300 are consistent with G2–G5. Between $\lambda 4000$ and $\lambda 4120$, HD 199178 (G5 IV) is an almost perfect spectral match (Fig. 1). The H γ line in HDE 283572 is too shallow to be as hot as G0, and G4 V and G5 V standards match most of the metallic lines. We conclude from this that G5 IV is a good estimate of the spectral type.

We have compared the UV continuum between 2400 and 3200 Å with those of G and K dwarf spectral standards as presented by Wu et al. (1983). The slope of the continuum is essentially the same as HD 161797 (μ Her, G5 IV). The stronger absorption features seen in the UV spectra also match well except for Mg II $\lambda\lambda$ 2800 and Mg I λ 2852. Finally, the UV flux level is matched very well by scaling the unreddened spectral standard to the visual magnitude of HDE 283572. We have also compared the UV continuum in HDE 283572 between λ 1700 and λ 2000 with stars of known spectral type; the shape of the continuum here is a sensitive measure of $T_{\rm eff}$. Again, the UV continuum of HDE 283572 is identical to that of HD 199178 (G5 IV). The continuum is cooler than G8 V (ξ Boo A) and G0 III (31 Com) and is similar to that of G2 IIIp (FK Com). The ultraviolet continuum is that of a G5 subgiant

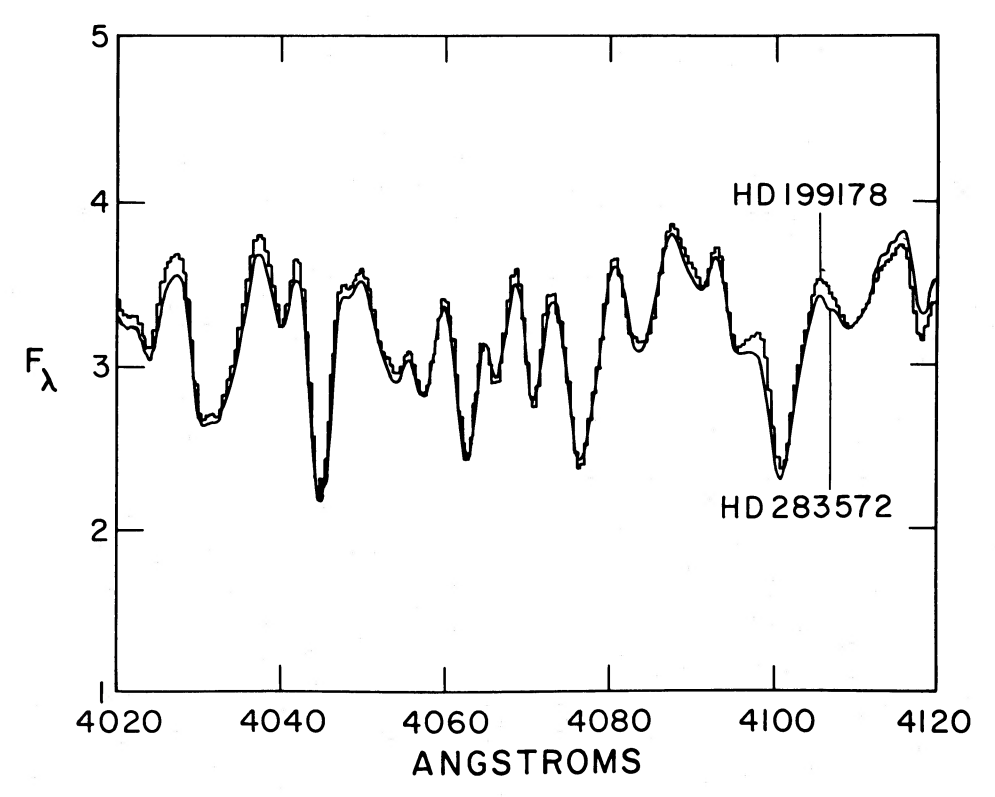


Fig. 1.—The mean IDS spectrum of HDE 283572 with a scaled superposed spectrum (the histogram) of HD 199178 (G5 IV). The flux scale is arbitrary. The line strengths reproduce quite well.

300

or about a K0 dwarf with no evidence for the UV continuum excess seen in many T Tauri stars.

With the exception of the U band, the mean colors are a good match to a G5–G8 giant, with maximum difference $\sim 0^{m}.08$ at L from a G5 III (Johnson 1966). The K-L color is $\sim 0^{m}.2$ too large for a K0 III and the BVR colors are too red for G0 III. At G5 III, HDE 283572 has a $\sim 0^{m}.1$ B excess and a $\sim 0^{m}.4$ U excess. There is no evidence for any IR excess. The U-B and B-V colors indicate $A_v \approx 0.3^{+0.2}_{-0.1}$.

Following Peterson and Carney (1979), we have used the $(R-I)_J$ and (V-K) colors to estimate $T_{\rm eff}$, finding $\log T_{\rm eff} = 3.68$ and 3.70, respectively, in good agreement with the G5 IV spectral type. The stellar angular diameter (Barnes and Evans 1976), from the V magnitude and V-R color corrected for extinction is 0.198 milli-arcsec (mas), which corresponds to 3.3 R_{\odot} at the assumed 160 pc distance of the Taurus T Association. This result, together with the photometric colors and the spectroscopy, imply an MK spectral type of G5 IV, with an uncertainty of about ± 2 subtypes.

b) Rotation

Inspection of the Lick coudé plate EC 16942 shows that the lines are broadened by rapid rotation. The lines near $\lambda 4000$ have a width of 115 km s⁻¹, which corresponds to $v \sin i \approx 95$ km s⁻¹ when the instrumental profile is removed. We estimate a 20% uncertainty in $v \sin i$. The FLWO and Oak Ridge spectra yield $v \sin i \approx 130$ km s⁻¹. These measurements imply a rotation period of $\sim 1^{45}$ sin i.

We have used the optical photometry obtained during 1983 October (Table 1) to search for rotational modulation of the stellar light caused by an asymmetric distribution of stellar surface brightness as is commonly seen in many other active stars (e.g., Rydgren and Vrba 1983). The V magnitude data are well described by a sinusoid with a peak-to-peak amplitude of 0^{m} 107 and a period of 1^{d} 548. The epoch of minimum light is JD 2,445,600.173. Figure 2a shows the sinusoidal fit to the observed V magnitudes, while the same data are plotted modulo the derived rotational period in Figure 2b. The RMS residual relative to the fitted sinusoid is ± 0.015 mag.

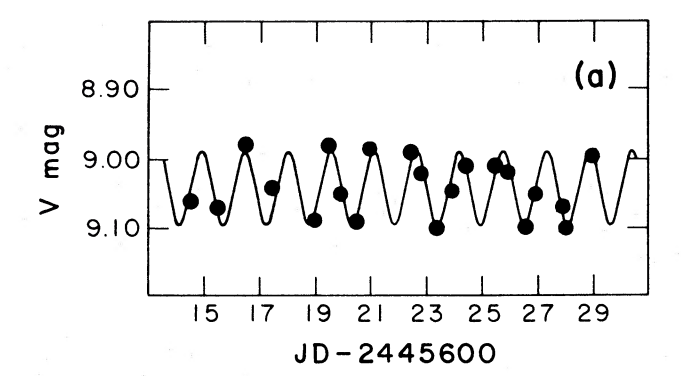
Unfortunately, the amplitude of the observed V magnitude variations is too small to permit a study of the associated color variations. Hence we cannot constrain the surface brightness inhomogeneities (starspots) which are presumably responsible for the photometric variability.

By analogy with other late-type stars with photometric periodicities, we interpret the 1.5 day photometric period as the axial rotation period of HD 283572. This period, combined with the stellar radius estimate derived above, implies an equatorial rotational velocity of 109 km s⁻¹, which is in excellent agreement with the spectroscopically derived $v \sin i$ values. It appears that we are observing this star nearly equator-on.

The contemporaneous UV continuum flux (obtained at phases 0.15, 0.4, 0.5, and 0.7) was also seen to vary. The amplitude of the variation in 100 Å intervals was greatest at 3000 Å (0.17 mag), decreasing to 0.05 mag at 2600 Å (see Table 4). The corresponding variation of V is 0.09 mag. The data are consistent with the expectation that the UV continuum varies in phase with the optical photometric variations.

c) Li I Abundance

The $\lambda 6707$ Li I resonance line in HDE 283572 is quite strong (Fig. 3) and is comparable in equivalent width to the $\lambda 6717$ Ca I feature. No other strong feature occurs near $\lambda 6707$, so we



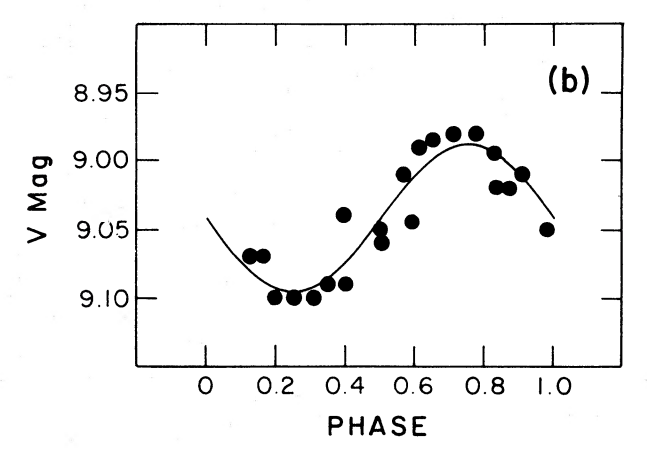


Fig. 2.—(a) The V magnitude observations during 1983 October, with the sinusoidal fit superposed. (b) The 1983 October V magnitudes folded on the orbital period. Within the errors (± 0.015 mag RMS) the shape of the light curve is sinusoidal.

assume that feature is predominantly Li I. The large equivalent width ($W_{\lambda} = 360 \pm 50$ mÅ) in a G star clearly indicates a large Li abundance, and a young age.

Following Zappala (1972), we have estimated a Li abundance of log $(N_{\rm Li})=2.8$, for $T_{\rm eff}=5000$ K and log $(N_{\rm H})=12.00$. We estimate an uncertainty of ± 0.1 dex, due mainly to the measurement uncertainty in $W_{\lambda}({\rm Li})$. This abundance is similar to that Zappala found in T Tauri stars. However, using the Li I curve of growth from D. Duncan (1982, private communication), $W_{\lambda}=360\pm50$ mÅ at 5000 K implies log $(N_{\rm Li})>3.3$. In either case, the abundances are essentially the cosmic abundances indicating that Li has not been significantly depleted in HDE 283572.

TABLE 4
UV CONTINUUM AND Mg II FLUXES

LWR	JD						
Image	(2,445,600+)	Phase	f_{2600}	f_{2700}	f_{2900}	f_{3000}	$f_{ m Mg~II}$
16946	15.894	0.16	4.02	6.06	11.54	13.52	109
16961	17.941	0.48	4.23	6.39	12.80	14.97	122
16971	20.942	0.42	4.15	6.55	12.76	15.75	128
16979	22.951	0.71	4.21	6.49	11.75	14.57	120

Note.— f_{λ} is the mean flux (units of 10^{-14} ergs cm⁻² s⁻¹ Å⁻¹) in the 100 Å bin centered at λ , and $f_{Mg,II}$ is the integrated flux in the Mg II h and k lines (units of 10^{-14} ergs cm⁻² s⁻¹), determined by differencing the spectra with that of HD 161797, a G5 IV spectral standard.

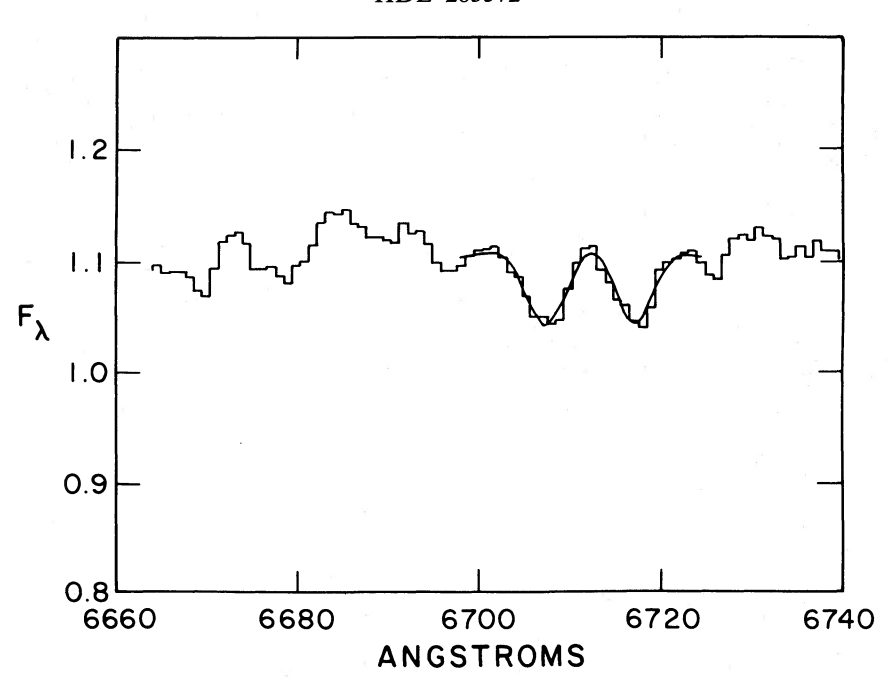


Fig. 3.—The Li I λ 6707 region. The feature at λ 6717 is due to Ca I. The superposed fit consists of two Gaussian absorption lines and a quadratic continuum. The lines are unresolved. The Li I λ 6707 equivalent width is 360 mÅ.

d) The Chromospheric Spectrum

A wide range of chromospheric emission lines are present in the *IUE* SWP-LO spectrum (Fig. 4). At longer wavelengths the Mg II and Ca II resonance doublets (Fig. 5) are prominently in emission. Identified chromospheric and transition region emission lines and their observed fluxes are listed in Table 5. There is no obvious H-Balmer emission.

The Ca II emission flux was measured by fitting a quadratic to the Ca II resonance absorption line and extrapolating beneath the emission reversal. At our low resolution this procedure should be fairly accurate. The mean observed surface flux in the K line is 1.6×10^6 ergs cm⁻² s⁻¹. The observed flux in the nine observations varies by $\pm 40\%$ from the mean. The 1983 October fluxes are constant to within about $\pm 10\%$ and are $\sim 40\%$ brighter than the 1982 fluxes. The two K line fluxes

301

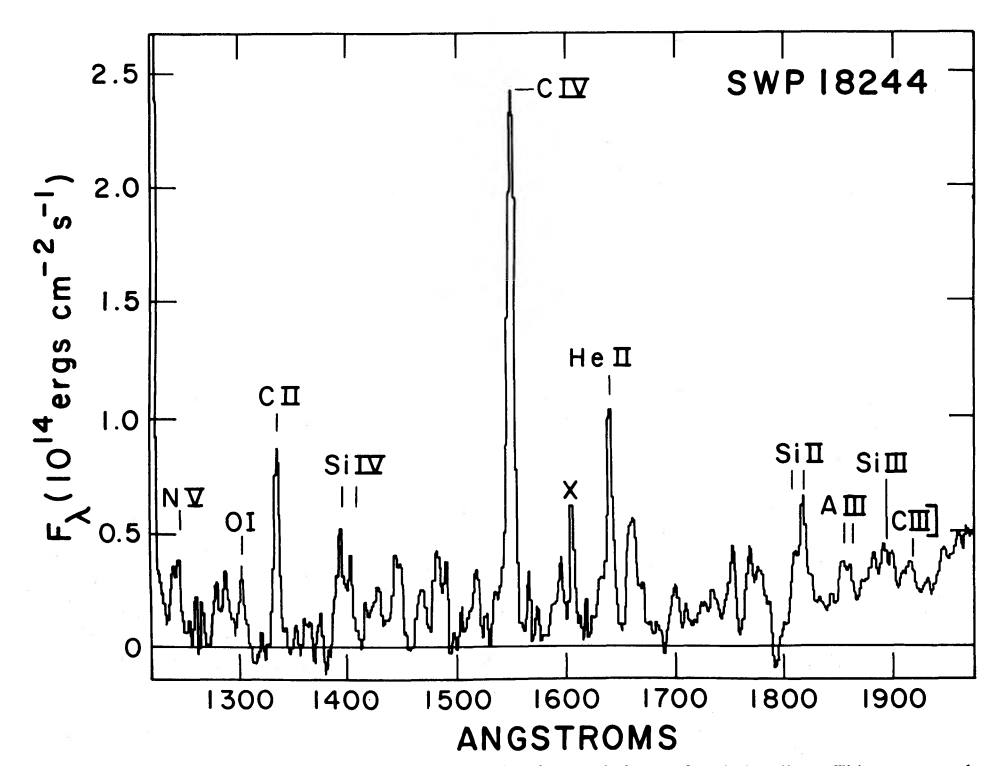


Fig. 4.—The low-resolution short-wavelength *IUE* spectrum SWP 18244, showing a plethora of emission lines. This spectrum has been smoothed with a Gaussian of 3 Å FWHM. Prominent lines are identified. The spectrum is qualitatively similar to that of most active chromosphere stars.

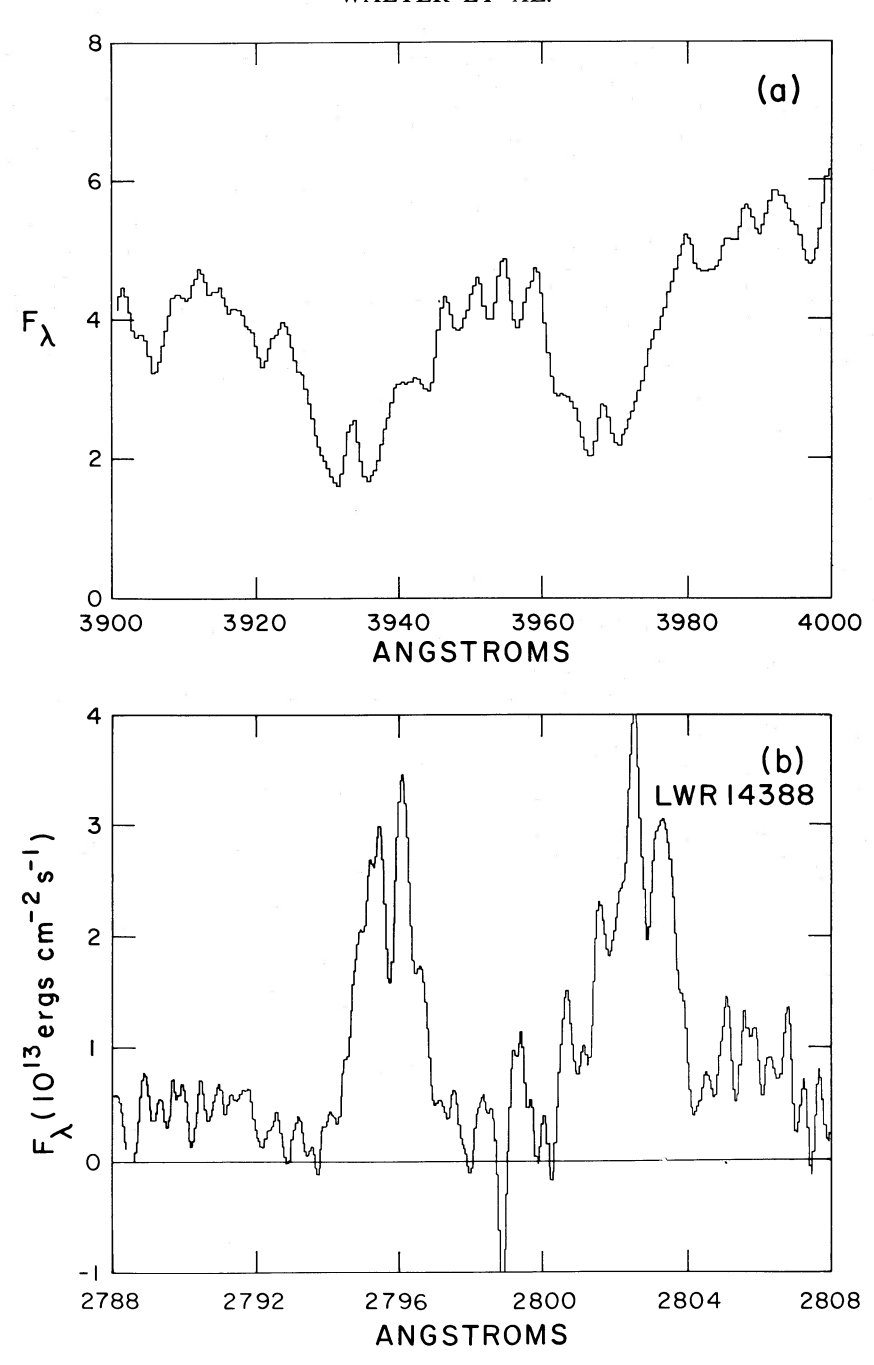


Fig. 5.—(a) A representative spectrum of the Ca II H and K resonance lines, obtained on 1985 October 21 using the KPNO 2^m 1 IIDS system. Spectral resolution is 1.7 Å. (b) The Mg II h and k lines, observed at high dispersion with the IUE on 1982 October 11 in a 240 minute exposure. The data have been smoothed with a Gaussian of width 0.2 Å. The lines are symmetric, with a prominent central reversal presumably attributable to interstellar absorption. The h line is very noisy because its location well off the peak of the echelle blaze.

in 1985 are \sim 20% fainter than in 1982. No phase-dependent variability is obvious. Long-term activity level changes are likely to dominate the variability of line fluxes.

The ratio of the flux in the K line to that in the H line (including any contribution from H ϵ) is 1.9 ± 0.4 , indicating the presence of significant H ϵ absorption. Subtraction of spectra of less active G dwarfs yields comparable residual emission fluxes in the H and K lines. The K line surface flux in HDE 283572 is comparable to those seen in the stars in Bopp's (1984) list of active stars.

The observed Mg II k surface flux is 4.2×10^6 ergs cm⁻² s⁻¹, with a k to h line flux ratio of unity. The absorption core absorbs $\sim 10\%$ of the emission. The line width (FWHM) is ~ 1.6 Å, which corresponds to v sin i=120 km s⁻¹ if entirely due to rotational broadening. The lines are symmetric, given the signal-to-noise ratio, and exhibit no evidence for blue-shifted absorption due to a stellar wind, unlike the case in many T Tauri stars (e.g., Penston and Lago 1983; Giampapa 1984; Brown, Ferraz, and Jordan 1984).

Mg II also is seen in emission in the low dispersion spectra.

No. 1, 1987 HDE 283572 303

TABLE 5

IDENTIFIED CHROMOSPHERIC AND TRANSITION
REGION EMISSION LINES

Species	λ	Observed Flux ^a
Са п Н	3968	12
Са п К	3933	23
Mg II h	2802	55
Mg II k	2795	53
N v	1240	$\leq 2.7^{b}$
О г	1304	2.2
С п	1335	5.3
Si IV	1393, 1402	6.2
Si 11	1527	≤0.52
C IV	1550	20.8
Не и	1640	5.5
C 1 + O III	1656 + 1663	4.9
N III	1750	≤2.7
Si 11	1808, 1817	6.1
Al II	1854, 1863	2.4
Si III	1892	2.2
С ін	1908	0.3

Note.—Surface fluxes can be obtained by multiplying the observed flux f by $\phi^2=4.4\times10^{18}$ and correcting for interstellar extinction.

Determination of the emission-line fluxes is made more difficult by the need to subtract the continuum. By matching the standard star spectrum (HD 161797) to the surrounding continuum, it is possible to subtract the standard absorption line profile from the HDE 283572 line, leaving just the Mg II emission contribution to the line. The mean of these observations yields a Mg II surface flux of 9.5×10^6 , within 10% of the h+k flux determined from the high-dispersion data in 1982 October. Variability with a range of $\sim 20\%$ is seen, similar to the Ca II data. Correcting for $E_{B-V}=0.1$ mag, the Mg II k/ Ca II k flux ratio is 2.7, which is similar to that observed in G dwarfs (Linsky $et\ al.\ 1982$).

The Mg I $\lambda 2851$ line appears weak in the low-dispersion spectra of HDE 283572 compared to the standard stars and is likely filled in by chromospheric emission. There is no evidence for any emission in the Balmer lines. H α and H γ through H9 are seen in absorption; a difference spectrum (HDE 283572–HD 199178) reveals no residual emission, and if anything, deeper H α absorption in HDE 283572. The Ca II infrared triplet was observed to be in absorption.

Aside from the usual chromospheric and TR lines, numerous, weak emission lines are clearly seen in the SWP spectrum and appear most likely to be low-excitation lines of species such as C I, Si II, S I, and Fe II. These lines are not present in comparably exposed spectra of G giants and dwarfs and may be due to the larger chromospheric emission measure of HDE 283572. Proper identification of these weak features will require higher signal-to-noise data.

We note that the N v feature is not the narrow, unresolved feature expected at IUE low resolution. Rather, there are clearly two peaks separated by 5 Å, at 1240 and 1245 Å. The lines are of comparable strength. This is similar to N v lines observed in other young G stars by Walter et al. (1984), who suggest the $\lambda 1240$ component is N v and the $\lambda 1245$ component is due to the confluence of C I lines ($\lambda\lambda 1243-1248$) observed in the solar spectrum. In determining the emission measure at log T=5.2, we have used the total observed flux: should the

longward component *not* be N v, the emission measure is overestimated by a factor of 2.

e) X-Rays

The X-ray source associated with HDE 283572 is extremely bright for a ninth-magnitude star, with $\log L_x/L_{\rm bol} = -3.0$, corresponding to $L_x = 2 \times 10^{31}$ ergs (0.1–4.1 keV at a distance of 160 pc). The X-ray surface flux is 3.0×10^7 ergs cm⁻² s⁻¹. Schrijver, Mewe, and Walter (1984) have fitted the X-ray spectrum from Einstein sequence 4507, finding $\log T_x = 7.41^{+0.84}_{-0.30}$ and $\log N_x \approx 21$. The best-fit temperature from the later observation (sequence 3843) is $\log T_x = 7.2$, with similar uncertainties. The specific emission measure $\int n_e dl = 10^{30.9} \text{ cm}^{-5}$ corresponding to a volume emission measure of $\sim 10^{54.7}$ cm⁻³ for a compact, isotropic corona at $\log T = 7.4$. The surface flux and emission measure are comparable to those seen in the most active RS CVn xystems, such as UX Ari and HR 1099 (Walter et al. 1980). There are no significant differences in the count rate or the source temperature between the two Einstein IPC observations. There was no significant variability during the individual observations on time scales of less than ~ 2000 s. The X-ray position agrees with the optical position to ~ 0.6 , which is well within the IPC spatial resolution.

No X-ray source was detected in the 7630 s EXOSAT CMA observation, with a 3 σ upper limit of 100 counts due to the high detector background off-axis. We folded the coronal spectrum derived from the IPC observations through the response function of the CMA with the thin Lexan filter, and we predict a count rate of 0.012 ± 0.003 counts s⁻¹ (for $N_x = 10^{21}$ cm⁻²), where the uncertainty is due to uncertainties in the spectral shape. Our prediction of 92 counts is less than the 3 σ upper limit and therefore, given the uncertainties in the spectrum, there is no discrepancy between the Einstein and EXOSAT data.

IV. CHROMOSPHERIC AND CORONAL STRUCTURE

a) Emission-Measure Distribution and Density Diagnostics

The emission-measure distribution of HDE 283572 was derived using the methods described by Jordan and Brown (1981), Brown, Ferraz, and Jordan (1984), and Brown et al. (1984). The emission measure of a collisionally excited, effectively thin emission line, $E_m = \int_{\Delta h} N_e^2 dh$, is related to the integrated line surface flux, F_* by

$$F_* = \frac{6.8 \times 10^{-22}}{\lambda \text{(cm)}} \frac{\Omega_{12}}{\omega_1} \frac{N_E}{N_H} \int_{\Delta h} N_e^2 g(T) dh ,$$

using a two-level atom for illustration. In cases involving metastable levels, the full population solution was included. Here Ω_{12} is the collision strength (Seaton 1962), ω_1 is the statistical weight of the lower level, and $N_{\rm E}/N_{\rm H}$ is the elemental abundance. The function g(T) is

$$g(T) = T_e^{-1/2} \exp\left(-\frac{W_{12}}{kT_e}\right) \frac{N_{\text{ion}}}{N_E},$$

where W_{12} is the excitation energy. The atomic data were as in Brown et al., except that the collision strengths and level populations of Lennon et al. (1985) were used for C II, of Berrington et al. (1981), and Kennan and Barrington (1985) for C III, and of Baluja, Burke, and Kingston (1981) and Dufton et al. (1983) for Si III. The elemental abundances were assumed to be solar, with values as in Brown, Ferraz, and Jordan.

a 10⁻¹⁴ ergs cm⁻² s⁻¹.

^b Total observed flux at 1240 and 1245 Å.

304

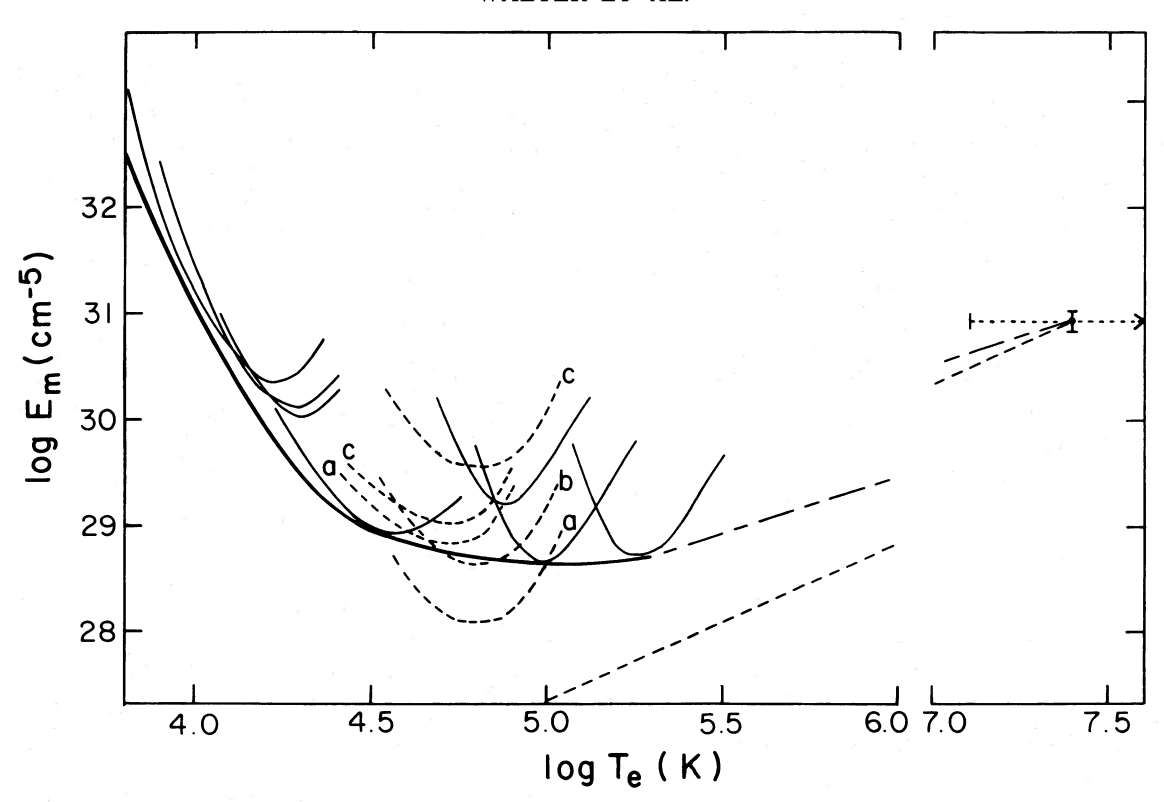


Fig. 6.—The emission-measure distribution for HDE 283572. Two possible distributions at intermediate temperatures are shown. Top: a linear interpolation between the X-ray and N v points. Bottom: an extrapolation from the X-ray point having an assumed $E_m \propto T_e^{3/2}$. Dashed lines: contribution functions for intersystem lines ("a", "b", and "c" indicate electron densities of 10^9 , 10^{10} , and 10^{11} cm⁻³, respectively).

The derived emission measures for the individual emission lines, corrected for an interstellar extinction of $E_{B-V} = 0.1$ using the average curve of Savage and Mathis (1979), are given in Table 6 along with the peak contribution temperature, T_m , for each line. For lines formed at cooler temperatures, the actual temperature of peak line formation will generally be lower than T_m because of the rapid rise in the emission-measure distribution. The mean emission-measure distribution, $E_m(T_e)$,

TABLE 6
ATOMIC DATA AND DERIVED EMISSION MEASURES

Ion	λ (Å)	F* corr	Ω	$g(T_m)$	N_E/N_H	E _m (cm ⁻⁵)	$\frac{\log T_m}{(K)}$
N v	1240	2.9 ^b	7.2	3.1(-4)	8.0(-5)	6.0(28)	5.2
C IV	1549	19.2	11.2	6.4(-4)	2.5(-4)	4.9(28)	5.0
Si IV	1396	6.0	16.4	2.2(-4)	4.0(-5)	1.7(29)	4.9
С III	1909	0.64	0.95	9.8(-4)	2.5(-4)	1.4(28)°	4.75
						$4.6(28)^{d}$	
						3.8(29)e	
Si 111	1892	1.95	3.2	8.5(-4)	4.0(-5)	7.4(28)°	4.7
				· ′	· ′	$7.8(28)^{d}$	
						1.2(29)e	
С п	1335	5.23	6.5	1.6(-4)	2.5(-4)	9.1(28)d	4.5
Si 11	1814	5.4	23	6.6(-5)	4.0(-5)	1.5(30)	4.3
	1526	0.48	1.7	2.9(-5)	· (1.2(30)	
Мд II	2800	113	35.4	2.6(-4)	4.0(-5)	2.5(30)	4.2

Note.— $g(T_m)$ is the value of g(T) at the peak of this function, where $T_e = T$.

a 10⁵ ergs cm⁻² s⁻¹.
 Determined using the total observed flux at 1240 and 1245Å. See text for details.

 $^{\circ} N_e = 10^9 \, \text{cm}^{-3}$.

 ${}^{d}N_{e} = 10^{10} \text{ cm}^{-3}.$ ${}^{e}N_{e} = 10^{11} \text{ cm}^{-3}.$ is shown in Figure 6. The contribution function, g(T), is shown for each line indicating the emission measure required at any particular temperature to produce the observed flux. For the C III and Si III intersystem lines the contribution functions appropriate for a range of electron density are presented.

The only density-sensitive line ratios available are Si III 1892 Å to C III 1909 Å $(3.1^{+0.6}_{-0.7})$, and Si IV 1393 + 1402 Å to C III 1909 Å $(9.3^{+2.3}_{-2.2})$, which, using the atomic data noted above, imply electron densities of $(2.1^{+0.5}_{-0.6}) \times 10^{10}$ cm⁻³ and $\leq (4.6^{+0.9}_{-1.4}) \times 10^{10}$ cm⁻³, respectively. The upper limit from the use of the Si IV lines arises from the likely presence of unresolved O IV lines in this emission feature. In addition, the emission-measure contribution curves for these lines provide an estimate of the electron density when compared with the derived mean emission-measure distribution. The curves for the Si III line are slightly high, but a reduction of $\sim 20\%$ in flux would bring these values into line with the mean emission measure while those for the C III line indicate a density just above 10^{10} cm⁻³. This level of agreement seems reasonable given the difficulties inherent in measuring the fluxes of these lines against the strong G-star continuum of HDE 283572.

b) Chromospheric and Transition Region Structure

The outer atmospheric structure of HDE 283572 was investigated using the modeling techniques described by Brown et al. (1984) and references therein. The electron pressure, P_e , is determined from the observed mean emission-measure distribution, $E_m(T_e)$, using

$$P_e^2 = P_0^2 + 2.8 \times 10^{-8} g_* \int_{T_e}^{T_0} E_m(T_e) dT_e$$
,

where P_0 and T_0 are the electron pressure and temperature at the top of the model and g_* is the stellar surface gravity, taken to be 5.0×10^3 cm s⁻². The modeling technique assumes hydrostatic equilibrium and, at least initially, spherical symmetry.

Models have been calculated using the previous equation for a range of P_0 and for two different $E_m(T_a)$ distributions, one based on the UV data alone (the thick solid line in Fig. 6) and the other based on a combination of the UV and X-ray data. A number of these models are shown in Figure 7. The first result which can be drawn from the modeling is that the combined UV and X-ray data cannot give a structure compatible with the density estimate derived earlier. This conclusion holds for any reasonable interpolation of the emission-measure distribution between the values derived from X-rays and the C IV and N v emission lines. If a 3/2 slope in log T is assumed, as suggested, for example, by the work of Jordan (1980) and Böhm-Vitense (1985), then the minimum scaled pressure (P_e/k) possible in the region of C III and Si III line formation is 5.2×10^{16} cm⁻³ K. If, however, the X-ray and N v emission measures are connected by a straight line, as in Figure 6, this minimum pressure becomes 6.8×10^{16} cm⁻³ K. Both values of P_e/k are clearly inconsistent with the observed value of $\sim 1.5 \times 10^{15}$ cm⁻³ K derived from the density-sensitive line ratios. With an additional assumption, it is possible to estimate the coronal density and pressure based on the X-ray data alone. If the emission arises in a spherically symmetric corona then

$$E_m(T_c) = \int_{\Delta R} N_e^2 dh \approx \overline{N_c^2} \Delta H ,$$

where $\overline{N_c^2}$ is the mean square coronal density and ΔH is the

isothermal scale height for the square of the density. Taking the observed values for $E_m(T_c)$ and T_c , the lower limit to the root-mean-square density is

$$(\overline{N_c^2})^{1/2} \ge 4.3 \times 10^9 \text{ cm}^{-3}$$

and the corresponding lower limit to the scaled pressure is

$$P_e/k \ge 1.1 \times 10^{17} \text{ cm}^{-3} \text{ K}$$
.

The most likely explanation for this discrepancy is that the X-ray and UV emissions come from physically distinct regions. One plausible situation is that the X-ray emission originates in high-density magnetically confined regions within a lower density atmosphere which would predominate in the UV emission lines. It seems likely that the X-ray-emitting regions are magnetically confined, given their very high temperature. A less likely explanation is that the X-ray data represent an abnormally high level of emission, i.e., a flare, but this would have to have been a relatively long-lived event, with little change in ~4 hr.

Models calculated from the UV data alone, with log $T_0 = 5.3$, are more in agreement with the density diagnostics. In this case the minimum pressure at log T = 4.75 is 1.1×10^{15} cm⁻³ K, which is close to the values derived from the density-sensitive line ratios, and suggests that little additional emission measure occurs above log $T_e > 5.3$.

c) Energy Balance and Requirements

An estimate of the chromospheric and transition region energy requirements can be obtained from the observed emission-measure distribution and the calculated atmospheric models. The radiative losses, ΔF_R , are determined directly

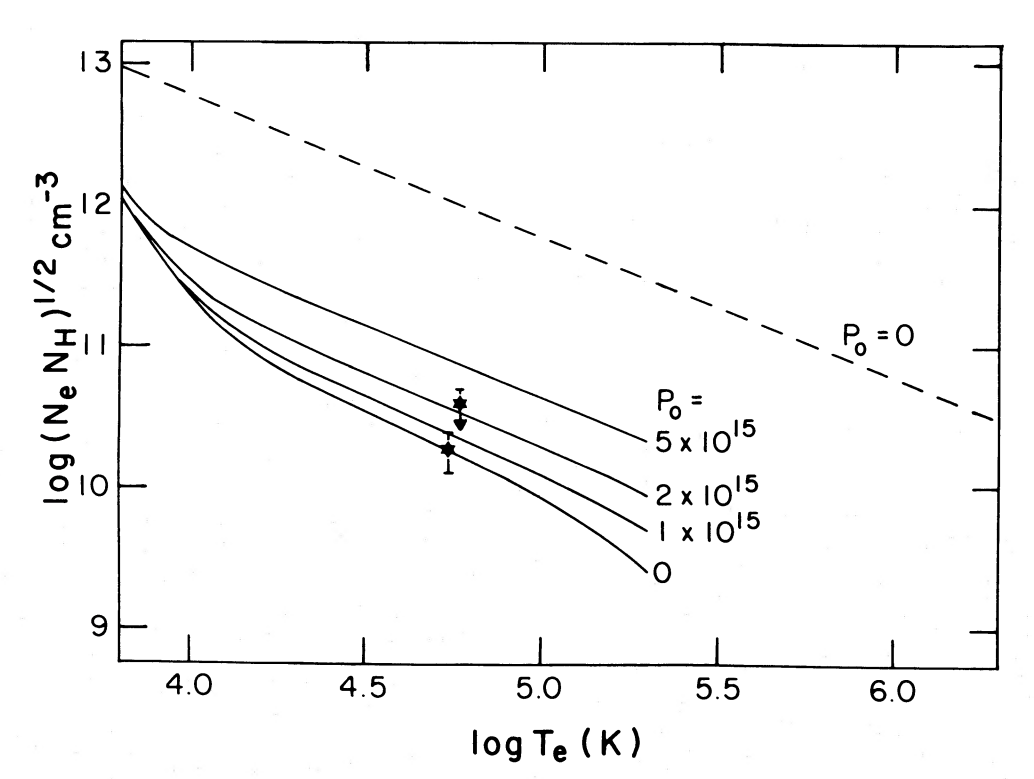


Fig. 7.—Models showing the variation of $(N_e N_H)^{1/2}$ with temperature. Solid lines: models based on the ultraviolet data alone (log $T_0 = 5.3$). Dashed line: a model combining the UV and X-ray data (log $T_0 = 7.2$). The stars show measured values of $(N_e N_H)^{1/2}$ obtained from the two density-sensitive line ratios.

TABLE 7

TERMS IN THE BALANCE FOR $P_0 = 1 \times 10^{15} \, \text{cm}^{-3} \, \text{K}$

$\log T_e $ (K)	$\log E_m \atop (\text{cm}^{-5})$	ΔF_R^{a}	$\Delta F_c^{\;a}$	F_m^{a}
3.9	31.78	3.9(7)		3.5(8)
4.0	31.09	8.9(7)		3.1(8)
4.1	30.50	9.7(7)		2.2(8)
4.2	29.96	5.9(7)		1.2(8)
4.3	29.51	1.7(7)		6.3(7)
4.4	29.19	5.7(6)		4.5(7)
4.5	28.98	3.2(6)		4.0(7)
4.6	28.87	2.6(6)		3.7(7)
4.7	28.80	3.5(6)	-1.1(2)	3.4(7)
4.8	28.74	5.8(6)	-1.5(2)	3.0(7)
4.9	28.70	6.5(6)	-1.8(2)	2.5(7)
5.0	28.68	6.2(6)	-1.9(2)	1.8(7)
5.1	28.68	5.9(6)	-1.6(2)	1.2(7)
5.2	28.70	6.2(6)	-1.8(2)	5.2(6)

a In ergs cm -2 s-1.

from the emission-measure distribution and, over an interval in $\log T_e$ of 0.3 dex, equal

$$\Delta F_R \approx 1.14 E_m(T_e) P_{\rm rad}$$
,

where $P_{\rm rad}$ is the power-loss function for which we have used the values of McWhirter, Thoneman, and Wilson (1975). The total radiative losses between the regions with log T_e from 4.0 to 5.3 are 3.1×10^8 ergs cm⁻² s⁻¹, which represent losses at a level of $\sim 10^3$ times the equivalent quiet Sun losses. While large, this level of radiative losses is still somewhat lower than those derived for active T Tauri stars (see, for instance, Brown, Ferraz, and Jordan 1984).

The thermal conductive flux, F_c , at any point in the atmosphere may be derived from the calculated models and is given by

$$F_c \approx -10^{-6} T_e^{5/2} \, \frac{dT_e}{dh} \, .$$

The net conductive flux, ΔF_c , may be either a source or sink term for any given region depending on the variation of the temperature gradient through the model.

At present, no evidence exists for substantial flows in the atmosphere of HDE 283572, and therefore we have assumed that energy transport and deposition by flows is negligible. Thus, the net input energy flux, ΔF_m , is that required to balance the net local energy transfer, i.e.,

$$\Delta F_m = \Delta F_R + \Delta F_c .$$

In Table 7 we present the energy balance terms for a model with $P_0 = 1 \times 10^{15} \text{ cm}^{-3} \text{ K}$ at log $T_0 = 5.3$ derived from an ultraviolet data alone. The conductive term is found to be negligible in this and all the other models derived from these ultraviolet data, and the required input mechanical energy in the upper chromosphere and transition region is essentially that required to balance the radiative losses. Without line profiles for the transition region emission lines it is not possible to progress further and investigate the possible modes of energy transport and deposition.

V. DISCUSSION

Clearly, HDE 283572 is an interesting object. It is probably very young, as evidenced by its Li abundance, its location in the HR diagram, and its spatial proximity to the Taurus-

Auriga star formation complex, yet it is not a T Tauri star. It does show the chromospheric and coronal flux levels expected in a young, rapidly rotating star. One could, of course, find an evolved star at the location in the H-R diagram occupied by HDE 283572 (log L = 0.8, log $T_e = 3.69$), by evolving a star of mass $M \approx 1.4 M_{\odot}$ (Iben 1967) for $\sim 3 \times 10^9$ yr. In this case the star would have been a mid-F star on the main sequence and the Li depletion time scale is long (Duncan 1981). However, the surface Li abundance is rapidly depleted during the H shell burning phase (Iben 1967), which might contradict the observed large Li abundance. Also, the chance of observing a star at this precise evolutionary phase within the physical boundaries of the Taurus-Auriga complex is very low. The proper motion $(\bar{\mu}_{\alpha} = 0.013 \text{ yr}^{-1}, \ \bar{\mu}_{\delta} = -0.026 \text{ yr}^{-1}; \ \text{B. F.}$ Jones 1981, private communication) and radial velocity (15 km s⁻¹) of HDE 283572 are consistent with a physical association with the Taurus Cloud (Jones and Herbig 1979; Herbig 1977). We conclude that it is highly unlikely that this star is a postmain-sequence object.

HDE 283572 lies near the base of the convective portion of the PMS evolutionary track for $M \approx 2~M_{\odot}$. On the basis of these tracks, HDE 283572 should be less evolved than the T Tauri star SU Aur and PMS stars like HP Tau G2 (Cohen and Kuhi 1979). Like HP Tau G2 (which is hotter, but on a similar radiative track), HDE 283572 exhibits no IR excess, but unlike HP Tau G2 there is no H α emission (see Fig. 23 of Cohen and Kuhi; in their Table 5 the entries for HP Tau G1 and G2 appear to be reversed). Were it not for its visual absorption of 2^m1, HP Tau G2 would have a similar apparent magnitude to HDE 283572. On the other hand, SU Aur, a more massive star, has strong H α emission, a large IR excess, and evidence for a strong stellar wind in its Mg II line profiles (cf. Giampapa 1984), all of which are absent in HDE 283572. The rapid rotation rate of HDE 283572 is similar to those observed by Vogel and Kuhi (1981) in PMS stars with $M \gtrsim 1.5~M_{\odot}$.

and Kuhi (1981) in PMS stars with $M \gtrsim 1.5~M_{\odot}$. HDE 283572 is a good example of a "naked" T Tauri (NTT) star (Walter 1986), as it differs from a classical T Tauri star primarily in the lack of significant amounts of circumstellar material and the accompanying IR and UV excesses and strong low excitation (H α , Ca II, and Mg II) emission lines. In this respect it is similar to the less massive NTT stars discussed by Mundt *et al.* (1983), Walter (1986), and Herbig, Vrba, and Rydgren (1986). It is likely that such stars have lost their T Tauri characteristics by dissipating their CS material, perhaps as a consequence of moving out of a dark cloud into a less dense environment of the ISM.

As discussed by Walter (1986), the NTT stars are common, with space densities comparable to those of the T Tauri stars. Because these stars are free of the complications introduced by the large CS envelopes of the classical T Tauri stars, these stars will be very useful as tests of stellar evolutionary calculations and for studies of how the *stellar* (not circumstellar) activity levels behave in very young convective stars.

VI. SUMMARY

HDE 283572 is a fairly massive ($\sim 2~M_{\odot}$) pre-main-sequence star associated with the Taurus-Auriga star formation complex. It exhibits few of the characteristics of the classical T Tauri stars and is a good example of a "naked" T Tauri star. The star is a mid-G subgiant, of $\sim 3~R_{\odot}$, rotating with a 1.45 period. The coronal and chromospheric surface fluxes are similar to those of the most active late type stars (excluding the T Tauri stars).

We thank the staffs of the Einstein Observatory, the IUE, the Lick Observatory, the Kitt Peak National Observatory, and the EXOSAT Observatory for their assistance in obtaining and reducing these data. We thank M. Tapia, L. Neri, and S. Saar for assistance in the photometric observations and reductions, G. Harlan for assistance in obtaining the coudé plate, and P.

Charles for obtaining and reducing the *EXOSAT* data. We are indebted to E. Feigelson for the Ca triplet observations and R. Mathieu for the high-resolution spectroscopy. We thank J. Barnes for her assistance with the KPNO data reductions. This research was supported by grants NAG8-508, NAG5-429, and NAG5-82 to the University of Colorado. The spectroscopic data were analyzed at the Colorado Regional Data Analysis Facility, which is supported by NASA grant NAG5-26409 and the GSFC Regional Data Analysis Facility. A. E. R. was partially supported by National Science Foundation grants AST 82-17851 and AST 84-19356. C. L. I. was partially supported by NASA contract NAG5-25774.

REFERENCES

Kennan, F. P., and Berrington, K. A. 1985, Solar Phys., 99, 25.
Lennon, D. J., Dufton, P. L., Hibbert, A., and Kingston, A. E. 1985, Ap. J., 294, 200.
Linsky, J. L., et al. 1982, Ap. J., 260, 670.
Linsky, J. L., Worden, S. P., McClintock, W., and Robertson, R. M. 1979, Ap. J. Suppl., 41, 47.
McWhirter, R. W. P., Thoneman, P. C., and Wilson, R. 1975, Astr. Ap., 40, 63.
Mundt, R., Walter, F. M., Feigelson, E. D., Finkenzeller, U., Herbig, G. H., and Odell, A. P. 1983, Ap. J., 269, 229.
Penston, M. V., and Lago, M. T. V. T. 1983, M.N.R.A.S., 202, 77.
Peterson, R. C., and Carney, B. W. 1979, Ap. J., 231, 762.
Ramsey, L. W., Barden, S. C., and Nations, H. L. 1980, Bull. A.A.S., 12, 836.
Robinson, L. B., and Wampler, E. J. 1972, Pub. A.S.P., 84, 161.
Roth, M., Iriarte, A., Tapia, M., and Resendiz, G. 1984, Rev. Mexicana Astr. Ap., 9, 25.
Rydgren, A. E., and Vrba, F. J. 1983, Ap. J., 267, 191.
Savage, B. D., and Mathis, J. S. 1979, Ann. Rev. Astr. Ap., 17, 73.
Schrijver, C. J., Mewe, R., and Walter, F. 1984, Astr. Ap., 138, 258.
Seaton, M. J. 1962, Proc. Phys. Soc. London, 79, 1105.
Vogel, S. N., and Kuhi, L. V. 1981, Ap. J., 245, 960.
Vrba, F. J., Rydgren, A. E., Chugainov, P. F., Shakovskaya, N. I., and Zak, D. S. 1986, Ap. J., 306, 199.
Walter, F. M. 1986, Ap. J., 306, 573.
Walter, F. M., Cash, W., Charles, P. A., and Bowyer, C. S. 1980, Ap. J., 236, 212.
Walter, F. M., Cash, W., Charles, P. A., and Bowyer, C. S. 1980, Ap. J., 236, 212.
Walter, F. M., Linsky, J. L., Simon, T. S., Vaiana, G. S., and Golub, L. 1984, Ap. J., 281, 815.
Wu, C.-C. 1983, NASA IUE Newsletter, No. 22, p. 1.
Wyatt, W. F. 1985, in Stellar Radial Velocities, ed. A. G. Davis Philip and D. W. Latham (Schenectady: L. Davis), p. 123.
Zappala, R. P. 1972, Ap. J., 172, 57.

A. Brown and J. L. Linsky: Joint Institute for Laboratory Astrophysics, University of Colorado, Boulder, CO 80309-0440

L. CARRASCO and M. ROTH: Instituto de Astronomia, Universidad Nacional Autónoma de Mexico, Apartardo Postal 70-264, Cuidad Universitaria, Mexico D.F., 04510, Mexico

P. F. CHUGAINOV and N. I. SHAKOVSKAYA: Crimean Astrophysical Observatory, p/o Nauchny, Crimea 334413, USSR

C. L. IMHOFF: Code 684.9, Goddard Space Flight Center, Greenbelt, MD 20771

A. E. RYDGREN: Boeing Aerospace Company, P.O. Box 3999, MS 87-08, Seattle, WA 98124-2499

F. Vrba: U.S. Naval Observatory, Flagstaff Station, P.O. Box 1149, Flagstaff, AZ 86002

F. M. Walter: Center for Astrophysics and Space Astronomy, University of Colorado, Boulder, CO 80309-0391